Theoretical study of light-emission properties of amorphous silicon quantum dots

Kengo Nishio* and Junichiro Kōga
Graduate School of Science and Technology, Keio University, 3-14-1 Hiyoshi, Kohoku-ku, Yokohama 223-8522, Japan

Toshio Yamaguchi
Department of Physics, Tokyo Women's Medical University, 8-1 Kawadacho, Shinjuku-ku, Tokyo 162-8666, Japan

Fumiko Yonezawa
Department of Physics, Keio University, 3-14-1 Hiyoshi, Kohoku-ku, Yokohama 223-8522, Japan
(Received 13 December 2002; published 5 May 2003)

In order to clarify the mechanism of the photoluminescence (PL) from amorphous silicon quantum dots (*a*-Si QDs), we calculate, in the tight-binding scheme, the emission spectra and the radiative recombination rate $\mathcal{P}$ of the direct band-to-band recombination process. For *a*-Si QDs smaller than 2.4 nm in diameter, our calculations beautifully reproduce the peak energy E_{PL} of the experimental PL peak [N.-M. Park *et al.*, Phys. Rev. Lett. **86**, 1355 (2001)]. Our analysis also show that (i) the emission energy can be tuned into the visible range of light from red to blue by controlling the sizes of *a*-Si QDs, and that (ii) $\mathcal{P}$ calculated for *a*-Si QDs is higher by two to three orders of magnitude than that for crystalline Si QDs. From these results, we assert that *a*-Si QDs are promising candidates for visible, tunable, and high-performance light-emitting devices.

DOI: 10.1103/PhysRevB.67.195304 PACS number(s): 71.23.−k, 61.46.+w, 78.66.Jg, 78.67.−n

I. INTRODUCTION

The idea of exploiting silicon (Si) for light-emitting devices is appealing because it leads to the possibility of fabricating light-emitting devices compatible with Si-based optoelectronic integrated circuits. When this idea is realized, device science will mark revolutionary progress since Si is a dominant material in present-day microelectronics technology. Bulk crystalline silicon (*c*-Si), however, is unsuitable for this purpose, because the band gap of *c*-Si is not only indirect but also near infrared. In this situation, the discovery in 1990 of efficient and visible photoluminescence (PL) from porous silicon and silicon nanocrystals has attracted much attention.[1,2]

Subsequent research from the theoretical side has shown that, accompanying the reduction in the sizes of *c*-Si nanostructures (NSs), (i) the type of the band gap transforms from indirect to direct, which increases the radiative recombination rate via a direct band-to-band recombination process, and (ii) the band-gap energy is blueshifted into the range of visible light owing to the quantum confinement effect.[3–5]

In a series of our recent papers, we have demonstrated that the radiative recombination rate becomes larger for nonsymmetric models than for symmetric models of *c*-Si NSs.[6–9] In particular, our results have confirmed that *c*-Si NSs of low symmetry reproduce the experimental relationship between the emission rate and energy, which *c*-Si NSs of high symmetry fail to explain.

As for amorphous silicon (*a*-Si) nanostructures, efficient visible PL had also been experimentally observed.[10–12] In spite of the fact that quite a few theoretical attempts[11,13–15] have been made to get a better understanding of emission properties, the mechanism of the PL from *a*-Si NSs is still an issue of controversy.

Recently, Park *et al.*[12] have observed efficient visible PL from *a*-Si quantum dots (QDs). They have suggested that, by controlling the sizes of *a*-Si QDs, it is possible to achieve PL over the range of visible light including red, green, and blue.

Three theoretical papers prior to the work of Park *et al.* calculated the emission energy of *a*-Si NSs. For instance, Estes and Moddel[13] used an extended version of the existing radiative recombination model proposed originally for bulk *a*-Si.[16] In their discussion, the electronic states of *a*-Si NSs are assumed to be the same as those of bulk *a*-Si and the blueshift of the emission energy is attributed to the purely geometrical effect in which the number of accessible localized states decreases accompanying the reduction of size. However, changes in electronic states from bulk *a*-Si to *a*-Si NSs cannot be ignored especially when the sizes of NSs are small. On the other hand, Allan, Delerue, and Lannoo[14,15] have taken into account changes in electronic states, and explained qualitatively the size dependence of the emission energy.

In order to make it possible to compare quantitatively the experimental data and theoretical results, the emission properties of *a*-Si NSs, on the basis of realistic structure models and reliable calculation methods for electronic states, must be determined. This is exactly the purpose of the present paper. By making use of our structure models and a tight-binding method, both to be described in what follows, the mechanism of light emission from *a*-Si NSs smaller than 2.4 nm in diameter is confirmed to be direct band-to-band recombination. We also show the superiority of *a*-Si QDs over *c*-Si QDs, concerning the emission properties, in the sense that (i) in the range of visible light, each desired color is realized by controlling the sizes of QDs, and (ii) the radiative recombination rate is higher, thus indicating the higher performance in luminescence.

II. MODEL AND METHOD

A. Model

Our principle for constructing structure models of *a*-Si QDs is to cut ellipsoids out of bulk *a*-Si. In this procedure of

model construction, it is vital to start from a high-quality structure model of bulk *a*-Si. For an excellent starting structure, we adopt the continuous random network (CRN) of bulk *a*-Si generated by Barkema and Mousseau.[17] Their CRN model is guaranteed in the sense that the radial distribution function (rdf) is in good agreement with the experimental rdf. Another advantage of their CRN model is that the electronic density of states of the model yields a well-defined band gap without any levels in the gap region.

Note that, even when the shapes of ellipsoids to be cut out are identical to one another, the atomic configuration varies from ellipsoid to ellipsoid because, in bulk *a*-Si, the environmental atomic distribution is different for different atoms. This is not the case for *c*-Si for which the atomic arrangement around each atom is always the same. Taking this fact into account, we construct 2000 different models of *a*-Si NSs by cutting 2000 ellipsoids for each set of axes $(2a,2b,2c)$, where $(2a,2b,2c)=$(2.4, 2.0, 1.6, and 1.2 nm). We define a "diameter" as $d\equiv 2\sqrt[3]{abc}$. We terminate surface dangling bonds with terminators in order to sweep out the surface states from the band gap.[18] In calculating a physical quantity, we take the average over these 2000 models, which improves the reliability of statistics.

B. Method

For our purpose, the calculation method must satisfy the following two requirements: (i) The computation speed to calculate the electronic states of each structure model must be considerably high, and (ii) the conduction band must be accurately described. The first requirement originates from the situation in which each model contains tens to hundreds of atoms and we have to deal with dozens of $(2a,2b,2c)$ sets where each set produces 2000 structure models. The second requirement is brought about by the fact that we are interested in optical properties which are evaluated by taking the sum of squared matrix elements between two states, each in the valence and conduction bands.

An empirical tight-binding (TB) scheme is a promising candidate for meeting the first requirement. By choosing the TB parameters carefully and including an appropriate number of atomic bases, the second requirement is also fulfilled. In practice, we use the $sp^3d^5s^*$ TB scheme proposed by Jancu *et al.*[19]

III. FORMULATION

In order to calculate emission properties, we first mention the radiative recombination rate via electric dipole transition $\mathcal{P}^{(i)}_{cn,vn'}$ between level n in the conduction band (c) and level n' in the valence band (v) of the ith structure model (*a*-Si QD), which is expressed as

$$\mathcal{P}^{(i)}_{cn,vn'}=\frac{1}{\tau^{(i)}_{cn,vn'}}=\frac{4n_0\alpha[E^{(i)}_{cn}-E^{(i)}_{vn'}]}{3m_e^2\hbar c^2}|\langle\psi^{(i)}_{cn}|p|\psi^{(i)}_{vn'}\rangle|^2, \tag{1}$$

where $\tau^{(i)}_{cn,vn'}$ is the radiative recombination time, n_0 is the refraction index (for which we set $n_0=1$), and α is the fine-structure constant. Parameters m_e, $\hbar$, and c are, respectively, the electron mass, the Planck constant divided by 2π, and the velocity of light. The momentum operator is denoted by p, and ψ_{cn} and $\psi_{vn'}$ represent the electronic wave functions n and n' in the conduction and valence bands, respectively, while $E^{(i)}_{cn}$ and $E^{(i)}_{vn'}$ are the corresponding energy levels. It must be noted that every quantity with the superscript (i) is concerned with the ith QD. The momentum matrix element $\langle\psi^{(i)}_{cn}|p|\psi^{(i)}_{vn'}\rangle$ is calculated by the scheme proposed in Ref. 20.

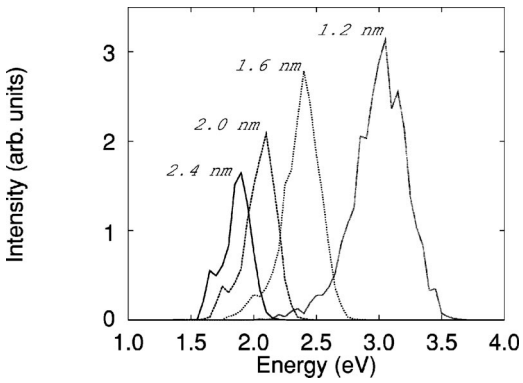

FIG. 1. Emission spectra of ellipsoidal *a*-Si QDs at 300 K versus emission energy. The four curves from left to right represent the results of *a*-Si QDs of 2.4, 2.0, 1.6, and 1.2 nm in diameter, respectively.

The emission spectrum is written, in terms of $\mathcal{P}^{(i)}_{cn,vn'}$, as

$$I(E)\propto\sum_i\left(\frac{\sum_{n,n'}\mathcal{P}^{(i)}_{cn,vn'}\exp\left\{-\frac{[E^{(i)}_{cn}-E^{(i)}_{vn'}]}{k_BT}\right\}}{\sum_{n,n'}\exp\left\{-\frac{[E^{(i)}_{cn}-E^{(i)}_{vn'}]}{k_BT}\right\}}\times\delta\{E-[E^{(i)}_{cn}-E^{(i)}_{vn'}]\}\right), \tag{2}$$

where the summation over n and n' is taken over all states contributing to the emission, and the summation over i covers all 2000 *a*-Si QDs for a given set of $(2a,2b,2c)$. The thermal average is defined by means of the Boltzmann weight.

IV. RESULTS

A. Emission-peak energy for *a*-Si QDs

In Fig. 1, the emission spectra $I(E)$ at $T=300$ K are presented for ellipsoidal *a*-Si QDs with four different sizes. As the diameter d decreases, the curve is blueshifted and becomes broader. We define the emission-peak energy E_{peak} by the energy at which $I(E)$ takes the maximum value.

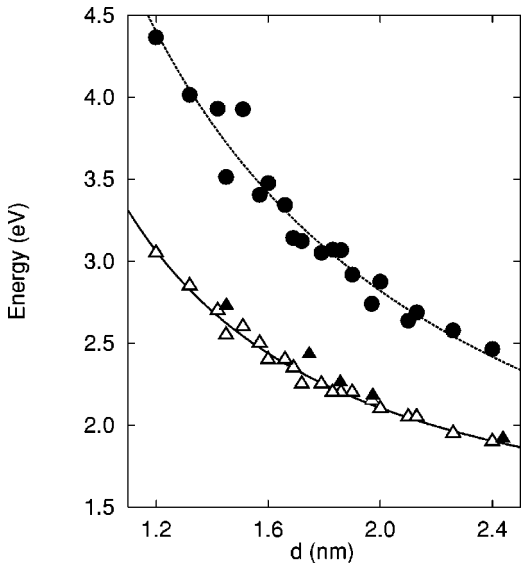

FIG. 2. Size dependence of the peak energy obtained from theoretical emission spectra of *a*-Si QDs (open triangles) and of *c*-Si QDs (filled circles) both at 300 K. The experimental PL peak energies reproduced from Ref. 12 (filled triangles) are given for the sake of comparison.

In Fig. 2, our results of E_{peak} (open triangles) are plotted against diameter d as defined in the above together with the experimental PL peak energy E_{PL} (filled triangles).[12] A different open triangle represents a different set of $(2a,2b,2c)$. The least-squares fit is shown by a solid curve to guide the eye. The emission-peak energy gradually increases, accompanying the decrease of diameter irrespective of the shape of the *a*-Si QD, the shape being characterized by $(2a,2b,2c)$. In the visible range of light from red ($\sim$1.85 eV) to blue ($\sim$2.64 eV), our result beautifully agrees with the experimental data. It must be emphasized that the radiative tunneling effect via band-tail states cannot account for the considerable change of emission energy, as shown in Fig. 2, according to the change of diameter d. It is also noted that the agreement with experiments comes about for our models in which the structure relaxation accompanying electron excitation is not taken into account, thus suggesting that the surface states play no important roles in the recombination. These facts altogether lead to our assertion that the origin of the photoluminescence in *a*-Si QDs in the size range smaller than 2.4 nm is the direct band-to-band recombination, related neither to tail states nor to surface states. Our result also predicts that even violet ($\sim$3.08 eV) is achieved when the size is reduced down to 1.2 nm. In other words, Fig. 2 indicates that the whole range of visible light is realized by controlling the sizes of *a*-Si QDs.

Allan, Delerue, and Lannoo[14] also calculated results similar to our results by means of the TB method which is again similar to our method. As a consequence, the results obtained by them and by the present paper are qualitatively similar. The difference lies in the quantitative nature. The emission energies evaluated in the present paper turn out to be higher than theirs. The origin of this difference is considered to be twofold:

(i) The amorphous structure we use here has been provided by Barkema and Mousseau,[17] in which the atomic configurations are made such that there appear no gap levels and accordingly the gap is clean and large enough.

(ii) In our calculations of the TB method, we have taken the atomic orbitals, $sp^3d^5s^*$,[19] which give a better description of the conduction band than that of the previous study where six atomic orbitals sp^3s^* (Ref. 21) are included.

B. Emission energy for *c*-Si QDs

For the sake of comparison, we evaluate the size dependence of the emission energy for *c*-Si QDs, which are constructed by cutting ellipsoids out of bulk *c*-Si and terminating the dangling bonds on the surface by terminators. For *c*-Si QDs, it is convenient to define the emission energy E_{emis} as follows:[15]

$$E_{\mathrm{emis}} \equiv \sum_i \left(\frac{\sum_{n,n'} [E_{cn}^{(i)} - E_{vn'}^{(i)}] \mathcal{P}_{cn,vn'}^{(i)} \exp\left\{ -\frac{[E_{cn}^{(i)} - E_{vn'}^{(i)}]}{k_{\mathrm{B}}T} \right\}}{\sum_{n,n'} \mathcal{P}_{cn,vn'}^{(i)} \exp\left\{ -\frac{[E_{cn}^{(i)} - E_{vn'}^{(i)}]}{k_{\mathrm{B}}T} \right\}} \right), \tag{3}$$

which is regarded as comparable with E_{peak} in the case of *a*-Si DQs. The emission energy E_{emiss} for *c*-Si QDs is also shown in Fig. 2 (filled circles) and the least-squares fit is also depicted by a solid curve. As in the case of *a*-Si QDs, the emission energy monotonically increases with decreasing size.

From Fig. 2, it is readily seen that the deviation of the emission energy from the value of a corresponding bulk system is smaller for *a*-Si than for *c*-Si. This result originates from the fact that the wave functions are more localized in *a*-Si than in *c*-Si, and accordingly the influence of quantum confinement is less remarkable in *a*-Si QDs.

C. Radiative recombination

The radiative recombination rate is the most important property in connection with the photoemission efficiency. If the radiative recombination rate is relatively high, a pair

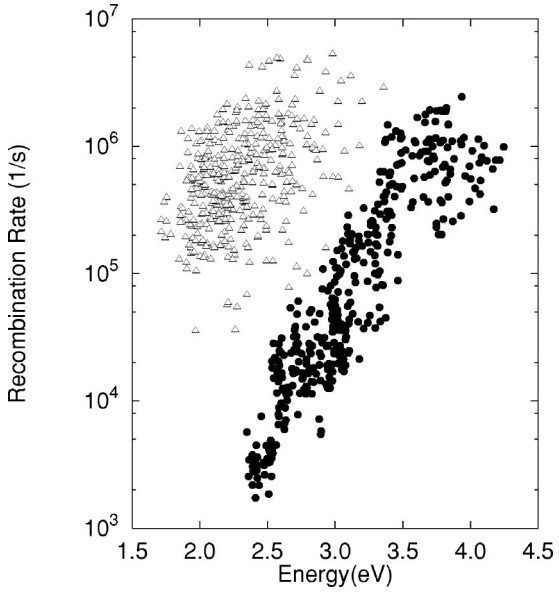

FIG. 3. The radiative recombination rate $\langle \mathcal{P} \rangle$ versus the emission energy at 300 K. The open triangles are results for *a*-Si QDs, while the filled circles are the results for *c*-Si QDs.

comprised of an excited electron and hole can recombine via the radiative emission process. If the radiative recombination rate is low, on the other hand, nonradiative recombination events degrade the performance of light emission.

We calculate the thermal average $\langle \mathcal{P} \rangle$ of the radiative recombination rate $\mathcal{P}^{(i)}_{cn,vn'}$, defined as[5]

$$\langle \mathcal{P} \rangle \equiv \langle \mathcal{P}^{(i)}_{cn,vn'} \rangle \equiv \sum_i \left(\frac{\sum_{n,n'} \mathcal{P}^{(i)}_{cn,vn'} \exp\left\{ -\frac{[E^{(i)}_{cn} - E^{(i)}_{vn'}]}{k_B T} \right\}}{\sum_{n,n'} \exp\left\{ -\frac{[E^{(i)}_{cn} - E^{(i)}_{vn'}]}{k_B T} \right\}} \right). \tag{4}$$

In Fig. 3, the averaged recombination rate $\langle \mathcal{P} \rangle$ is plotted against the emission energy both for *a*-Si QDs (open triangles) and for *c*-Si QDs (filled circles), which shows that $\langle \mathcal{P} \rangle$ for *a*-Si QDs is larger by two to three orders of magnitude than that for *c*-Si QDs.

This enormous difference between $\langle \mathcal{P} \rangle$ for *a*-Si QDs and *c*-Si QDs is explained from the definition of $\mathcal{P}^{(i)}_{cn,vn'}$ in Eq. (1). When *m* is supposed to stand for either *n* or n' describing the electronic state in the conduction (c) or valence (v) band, and b stands for either c or v, the wave function $|\psi_{bm}\rangle$ is expanded in terms of the atomic wave functions $|k\mu\rangle$ as $|\psi_{bm}\rangle = \Sigma_{k\mu} a_b(m{:}k\mu)\ |k\mu\rangle$ where *k* denotes the atomic site, μ describes the angular momentum, and $a_b(m{:}k\mu)$ is the expansion coefficient. The matrix element in Eq. (1), therefore, is written, with *k* as the site and μ as angular momentum, as

$$\langle \psi_{cn} | p | \psi_{vn'} \rangle = \sum_{k\mu,\ell\nu} a^*_c(n{:}k\mu) a_v(n'{:}\ell\nu)\ \ \langle k\mu | p | \ell\nu \rangle, \tag{5}$$

which indicates that when the atomic configuration in the QD under consideration has high symmetry, as in the case of a *c*-Si QD, there appears, on the right-hand side of Eq. (1), a number of pairs, in each of which the two terms have the same absolute value with opposite signs and consequently cancel each other out.[8] In the case of an *a*-Si QD, there exist no such pairs, and as a result all the terms contribute to $\mathcal{P}^{(i)}_{cn,vn'}$, thus making the resultant value much larger. A tendency similar to this was suggested in Ref. 14. Our results presented in Fig. 3 indicate that *a*-Si QDs are superior to *c*-Si QDs in luminescence efficiency.

V. SUMMARY

In summary, we have studied the emission properties of *a*-Si QDs with the CRN structure model and $sp^3d^5s^*$ tight-binding scheme. We have demonstrated theoretical evidence that the emission energy of *a*-Si QDs can be tuned, by controlling the sizes, in the visible range of light from red to violet. Our result for the emission-peak energy beautifully reproduces experimental data, which strongly suggests that the origin of PL from *a*-Si QDs in the size region smaller than 2.4 nm is the direct band-to-band recombination. Our results also show that the radiative recombination rate for *a*-Si QDs is much larger than that for *c*-Si QDs. On the basis of these results, we assert that *a*-Si QDs are promising candidates for visible, tunable, and high-efficiency light-emitting devices.

ACKNOWLEDGMENTS

We are grateful to G. T. Barkema and Normand Mousseau for providing us with the coordinates of the continuous random network model.

*Email address: knishio@rk.phys.keio.ac.jp

[1] L. T. Canham, Appl. Phys. Lett. **57**, 1046 (1990).
[2] H. Takagi, H. Ogawa, Y. Yamazaki, A. Ishizaki, and T. Nakagiri, Appl. Phys. Lett. **56**, 2379 (1990).
[3] J. P. Proot, C. Delerue, and G. Allan, Appl. Phys. Lett. **61**, 1948 (1992).
[4] G. D. Sanders and Y. Chang, Phys. Rev. B **45**, 9202 (1992).
[5] C. Delerue, G. Allan, and M. Lannoo, Phys. Rev. B **48**, 11024 (1993).
[6] J. Kōga, K. Nishio, H. Ohtani, T. Yamaguchi, and F. Yonezawa, J. Phys. Soc. Jpn. **69**, 2188 (2000).
[7] J. Kōga, K. Nishio, T. Yamaguchi, and F. Yonezawa, J. Phys. Soc. Jpn. **70**, 2478 (2000).
[8] J. Kōga, K. Nishio, T. Yamaguchi, and F. Yonezawa, J. Phys. Soc. Jpn. **70**, 3143 (2001).
[9] J. Kōga, K. Nishio, H. Ohtani, T. Yamaguchi, and F. Yonezawa, J. Non-Cryst. Solids **293-295**, 630 (2001).
[10] E. Bustarret, M. Ligeon, and L. Ortéga, Solid State Commun. **83**, 461 (1992).
[11] R. B. Wehrspohn, J.-N. Chazalviel, F. Ozanam, and I. Solomon, Eur. Phys. J. B **8**, 179 (1999).

[12] N.-M. Park, C.-J. Choi, T.-Y. Seong, and S.-J. Park, Phys. Rev. Lett. **86**, 1355 (2001).
[13] M. J. Estes and G. Moddel, Appl. Phys. Lett. **68**, 1814 (1996).
[14] G. Allan, C. Delerue, and M. Lannoo, Phys. Rev. Lett. **78**, 3161 (1997).
[15] G. Allan, C. Delerue, and M. Lannoo, Appl. Phys. Lett. **71**, 1189 (1997).
[16] D. J. Dunstan and F. Boulitrop, Phys. Rev. B **30**, 5945 (1984).
[17] G. T. Barkema and N. Mousseau, Phys. Rev. B **62**, 4985 (2000).
[18] K. Nishio, J. Kōga, H. Ohtani, T. Yamaguchi, and F. Yonezawa, J. Non-Cryst. Solids **293-295**, 705 (2001).
[19] J.-M. Jancu, R. Scholz, F. Beltram, and F. Bassani, Phys. Rev. B **57**, 6493 (1998).
[20] L. Brey and C. Tejedor, Solid State Commun. **48**, 403 (1983).
[21] P. Vogl, H. P. Hjalmarson, and J. D. Dow, J. Phys. Chem. Solids **44**, 365 (1983).